

Andreev reflection in altermagnets

Chi Sun,¹ Arne Brataas,¹ and Jacob Linder¹

¹Center for Quantum Spintronics, Department of Physics, Norwegian University of Science and Technology, NO-7491 Trondheim, Norway

Recent works have predicted materials featuring bands with a large spin-splitting distinct from ferromagnetic and relativistically spin-orbit coupled systems. Materials displaying this property known as altermagnets, featuring a spin-polarized band structure reminiscent of a d -wave superconducting order parameter. We here consider the contact between an altermagnet and a superconductor and determine how the altermagnetism affects the fundamental process of Andreev reflection. We show that the resulting charge and spin conductance depends strongly on the interfacial orientation of the altermagnet relative to the superconductor. The topological zero-energy states present at the interface in the d -wave case are robust toward the presence of an altermagnetic interaction. Moreover, the spin conductance can be increased by more than an order of magnitude compared to its normal-state value and also changes its sign via the applied bias voltage. These results show how the spin-anisotropic altermagnetic state can be probed by conductance spectroscopy, and how it offers voltage-control over directionally dependent spin currents that are strongly enhanced due to superconductivity.

Introduction. The interaction between magnetism and superconductivity is a major research topic in modern condensed matter physics [1–4]. Its allure stems both from a fundamental viewpoint and cryogenic technology applications such as extremely sensitive detectors of radiation and heat as well as circuit components such as qubits and dissipationless diodes [5, 6].

To understand the transport of charge, spin, and heat in such structures, it is crucial to understand the basic transport mechanism involving the Cooper pair condensate: Andreev reflection [7]. Whereas Andreev reflection in ferromagnet materials has been studied in great detail [3], antiferromagnetic materials has received less attention. A particularly interesting example is recently discovered antiferromagnets [8, 9] that break time-reversal symmetry and feature a spin-splitting that does not originate from relativistic effects such as spin-orbit coupling [10]. Dubbed altermagnets [11] in the literature, these are spin-compensated magnetic systems with a huge momentum-dependent spin splitting even in collinearly ordered antiferromagnets. *Ab initio* calculations have identified several possible material candidates that can host an altermagnetic state, including metals like RuO₂ and Mn₅Si₃ as well as semiconductors/insulators like MnF₂ and La₂CuO₄ [12–16].

There exists an interesting analogy between altermagnets and unconventional superconductivity in the high- T_c cuprates where the order parameter has a d -wave symmetry in momentum space [17]. Similarly, the band structure of altermagnets has a spin-resolved d -wave symmetry which mimicks the structure of the d -wave superconducting order parameter (see Fig. 1). Since hybrid structures of superconductors and magnetic materials are attracting wide interest due to their functional properties, we here consider Andreev reflection in an altermagnet (AM)/superconductor (SC) bilayer. We allow for both conventional s -wave superconductivity and unconventional d -wave superconductivity. Importantly, we allow for different crystallographic orientations of the interface between the materials to explore both how the nodal orientation of the SC order parameter and the spin-resolved Fermi surface orientation in the AM affect transport.

We find that the altermagnetism strongly influences both charge and spin currents flowing into the SC for high-transparency contacts. Depending on the crystallographic orientation of the interface relative to the spin-polarized lobes of the altermagnetic Fermi surface, the zero-bias charge conductance peak in d -wave superconductors can be either enhanced or suppressed with increasing altermagnetic strength. Moreover, the spin conductance is highly tunable via the applied bias voltage. This includes a sign reversal of the spin current when the SC features a d -wave symmetry. Our findings demonstrate how the unique momentum-dependent spin polarization of the altermagnetic state is revealed in conductance spectroscopy, and how it offers voltage-control over directionally dependent spin currents.

Theory. The Hamiltonian for the AM, using a field operator basis $\psi = [\psi_\uparrow, \psi_\downarrow, \psi_\uparrow^\dagger, \psi_\downarrow^\dagger]$, is given by

$$\hat{H}_{\text{AM}} = \begin{pmatrix} \underline{H}_{\text{AM}} & 0 \\ 0 & -\underline{H}_{\text{AM}}^* \end{pmatrix}, \quad \underline{H}_{\text{AM}} = -\frac{\hbar^2 \nabla^2}{2m_e} - \mu + \alpha k_x k_y \sigma_z, \quad (1)$$

in which α is the parameter characterizes the altermagnetism strength, σ_z denotes the Pauli matrix, m_e is the electron mass, μ is the chemical potential and \dots is notation for a 2×2 matrix. The four eigenpairs are obtained as: $E_1 = E_+$ with $(1, 0, 0, 0)^T$ for $e \uparrow$, $E_2 = E_-$ with $(0, 1, 0, 0)^T$ for $e \downarrow$, $E_3 = -E_+$ with $(0, 0, 1, 0)^T$ for $h \uparrow$ and $E_4 = -E_-$ with $(0, 0, 0, 1)^T$ for $h \downarrow$, using e/h for electron/hole excitations. The eigenenergies are $E_\pm = \frac{\hbar^2(k_x^2 + k_y^2)}{2m_e} - \mu \pm \alpha k_x k_y$.

Considering an excitation with energy E , the x -components of the four possible wave vectors in the AM are given by $k_{e(h)\sigma, \pm} = \pm \hbar^{-1} \sqrt{2m_e(\mu \pm E) - \hbar^2 k_y^2 + \alpha^2 m_e^2 k_y^2 \hbar^{-2} - \alpha \sigma m_e k_y \hbar^{-2}}$, where $\sigma = +1(-1)$ for spin- $\uparrow(\downarrow)$, $\pm' = +(-)$ for $e(h)$. The \pm sign in the subscript denotes propagation direction along $\pm x$. Translational invariance is assumed in the y -direction with belonging momentum k_y of the incident particle. In the superconducting region, we use well-known expressions for the Hamiltonian and eigenenergies/states, allowing for both an s -wave and d -wave symmetry (see SM for details).

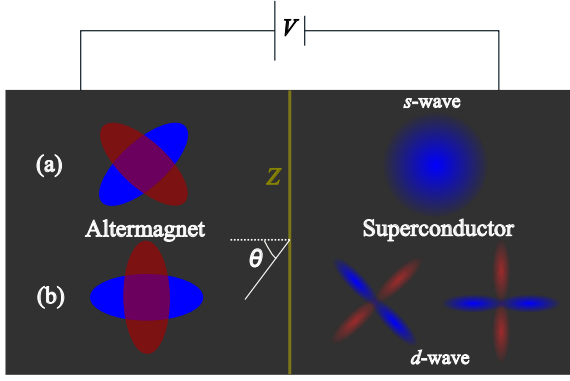


FIG. 1. Andreev reflection is probed in a bilayer consisting of an altermagnet (AM) and a superconductor (SC). The order parameter in the SC can have a s -wave or d -wave symmetry, including different nodal orientations of the d -wave case. Different interface orientations are also considered, effectively rotating the spin-resolved Fermi-surface in the AM for majority (blue ellipse) and minority (red ellipse) spin carriers. A voltage V is applied to the system and the differential conductance provides information about the Andreev reflection.

The altermagnetic Hamiltonian modifies the standard expressions for the charge current and boundary conditions satisfied by the scattering wavefunctions. To see this, consider for concreteness an $e \uparrow$ incident from the AM side of an AM/SC bilayer, we have

$$\begin{aligned} \Psi_{AM,e\uparrow} &= \begin{pmatrix} 1 \\ 0 \end{pmatrix} e^{ik_{e\uparrow,x}} + r \begin{pmatrix} 1 \\ 0 \end{pmatrix} e^{ik_{e\uparrow,-x}} + r_A \begin{pmatrix} 0 \\ 1 \end{pmatrix} e^{ik_{h\uparrow,x}}, \\ \Psi_{SC,e\uparrow} &= t \begin{pmatrix} u_+ \\ v_+ e^{-i\gamma_+} \end{pmatrix} e^{iq_{e,+x}} + t_A \begin{pmatrix} v_- e^{i\gamma_-} \\ u_- \end{pmatrix} e^{-iq_{h,-x}}, \end{aligned} \quad (2)$$

in which r , r_A , t and t_A describe the normal reflection, Andreev reflection, normal transmission and Andreev transmission, respectively. We consider a superconducting gap which can be anisotropic, $\Delta = \Delta_0 g(\theta_S)$ with $g(\theta_S) = 1$ for the s -wave case and $g(\theta_S) = \cos(2\theta_S - 2\beta)$ for the d -wave case, where $e^{i\gamma_{\pm}} = g(\theta_{\pm})/|g(\theta_{\pm})|$ with $\theta_+ = \theta_S$ and $\theta_- = \pi - \theta_S$ are defined. The scattering angle θ_S in the SC is determined from θ in the AM by using conservation of momentum k_y .

To derive the boundary condition for the $e \uparrow$ incident, antisymmetrization of the altermagnetic term $\alpha k_x k_y \sigma_z \rightarrow \frac{\alpha k_y}{2} \{k_x, \Theta(-x)\} \sigma_z$ is necessary to ensure hermiticity of the Hamilton-operator. Above, $k_x = -i\partial_x$. Applying $H\Psi = E\Psi$ and integrating over $[-\epsilon, \epsilon]$ with $\epsilon \rightarrow 0$, we obtain $\Psi_{AM,e\uparrow}|_{x=0} = \Psi_{SC,e\uparrow}|_{x=0} = (f, g)^T$ and

$$\partial_x \Psi_{SC,e\uparrow}|_{x=0} - \partial_x \Psi_{AM,e\uparrow}|_{x=0} = \begin{pmatrix} k_{\alpha,+1} f \\ k_{\alpha,-1} g \end{pmatrix}, \quad (3)$$

where $k_{\alpha,\sigma} = \frac{2m_e}{\hbar^2} (U_0 + \frac{i\alpha k_y \sigma}{2})$. The boundary conditions for incident $e \downarrow$, $h \uparrow$ and $h \downarrow$ particles can be found in the SM.

To compute the conductance of the junction, the charge current produced by all possible types of incoming quasiparticles toward the interface must be taken into account. The

electric current is computed by taking the quantum mechanical expression for the charge current and multiplying with the density of states (DOS) and distribution function of the incident particle. The DOS of quasiparticles in the superconducting region is well-known, but is worth presenting in the altermagnetic region. We consider again an incident $e \uparrow$ with energy E from the AM side for concreteness. We have $E = E_+ = \frac{\hbar^2(k_x^2 + k_y^2)}{2m_e} - \mu + \alpha k_x k_y$. The general expression for 2D DOS of a band $E(\mathbf{k})$ is given by

$$N(E) = \frac{1}{4\pi^2} \int \frac{dl}{|\nabla_{\mathbf{k}} E(\mathbf{k})|}, \quad (4)$$

which can be used to compute the \mathbf{k} -anisotropic DOS in the altermagnetic case. When $\alpha < \hbar^2/m_e \equiv \alpha_c$, a constant energy contour defines an elliptical energy surface in \mathbf{k} -space for spin- \uparrow electrons. The ellipse has semi-major (minor) axis $a(b)$, which can be obtained as $a = \sqrt{\frac{2m_e(\mu+E)}{\hbar^2 - m_e \alpha}}$, $b = \sqrt{\frac{2m_e(\mu+E)}{\hbar^2 + m_e \alpha}}$. On the other hand, when $\alpha > \alpha_c$, the energy dispersion corresponds to a hyperbola, which can not define a closed integral path. Therefore, we confine $\alpha < \alpha_c$ in this work.

Using Eq. (4), we have $N(E) = \int_0^{2\pi} N(E, \theta) d\theta$ with

$$N(E, \theta) = \sqrt{\frac{(dk_x/d\theta)^2 + (dk_y/d\theta)^2}{16\pi^4 [(\hbar^2 k_x m_e^{-1} + \alpha k_y)^2 + (\hbar^2 k_y m_e^{-1} + \alpha k_x)^2]}}, \quad (5)$$

where $k_{x,y}$ are the coordinates on the elliptical Fermi surface of the $e \uparrow$ incident at a given angle θ .

The quantum mechanical charge current density for $e \uparrow$ channel in the AM is given by

$$j_{Q,e\uparrow} = -\frac{e\hbar}{m_e} \{ \Im m \{ f^* \nabla f \} + \Im m \{ g^* \nabla g \} \} - \frac{e\alpha k_y}{\hbar} (|f|^2 - |g|^2). \quad (6)$$

Using Eq. (6), we can compute the total charge current flowing in the $e \uparrow$ channel in the AM. Assume that a voltage is applied across the AM/SC junction so that the distribution function for electrons [holes] is $f(E - eV)$ [$f(E + eV)$] on the AM side while it is $f(E)$ for quasiparticles on the SC side. For instance, an incoming hole from the AM side can be Andreev-reflected into the $e \uparrow$ channel as $\psi = r_A \begin{pmatrix} 1 \\ 0 \end{pmatrix} e^{ik_{e\uparrow,-x}}$ and contributes with a current $J_{Q,e\uparrow} = -e N_{h\downarrow,-}^{AM}(E, \theta) |r_A|^2 f(E + eV) (\frac{\hbar k_{e\uparrow,-}}{m_e} + \frac{\alpha k_y}{\hbar})$. Here $N_{h\downarrow,-}^{AM}(E, \theta)$ is the DOS in the AM for $E = -E_-$ and $k_x = k_{h\downarrow,-}$, which can be obtained by following the same procedure as described above.

The total charge current I is finally obtained by first computing the total electric current flowing in the e and h channels for both spins on the AM side, each contribution determined by $j_{Q,i} f_i(E) N_i(E)$ where $j_{Q,i}$ is the charge current $I(V)$ produced by an incoming particle channel i , $f_i(E)$ is the distribution function for channel i , and $N_i(E)$ is the DOS for channel i , and then integrating over all possible angles of incidence

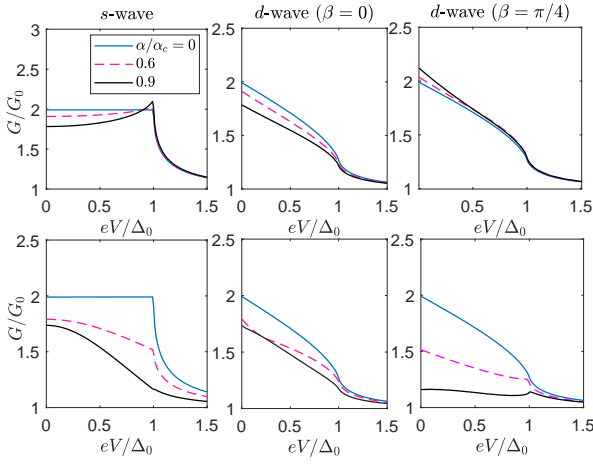


FIG. 2. (Color online) Normalized charge conductance G/G_0 as a function of bias voltage for different types of AM/SC junctions. The barrier is set to $Z = 0$, which describes a high-transparency contact. The columns correspond to different superconducting order parameter symmetries. *Upper row*: case (a) in Fig. 1 [AM term $\alpha k_x k_y$ in \underline{H}_{AM}]. *Lower row*: case (b) in Fig. 1 [AM term $\alpha(k_x^2 - k_y^2)/2$ in \underline{H}_{AM}].

θ through $\int dk_y = \int (dk_y/d\theta)d\theta$. The conductance is then $G(V) = dI/dV$ and we normalize it against the high-voltage conductance (normal-state) $G_0 = \lim_{eV \gg \Delta_0} G(V)$. The spin current I_S is obtained by computing the difference between the currents carried by spin- \uparrow and spin- \downarrow excitations, and the spin conductance is $G_S = dI_S/dV$ with a similar normalization as for the charge current.

We will show how the conductance of the AM/SC junction depends strongly on the crystallographic orientation of the interface between the materials. This can be modelled by replacing $\alpha k_x k_y \rightarrow \alpha(k_x^2 - k_y^2)/2$ in \underline{H}_{AM} , corresponding to a 45 degree rotation of the interface. This leads to different expressions for the wavevectors $k_{e(h)\sigma,\pm} = \pm \sqrt{\frac{2m_e(\mu \pm E + \sigma \alpha k_y^2/2) - \hbar^2 k_x^2}{\hbar^2 + m_e \sigma \alpha}}$, boundary condition

$$\partial_x \Psi_{SC,e\uparrow}|_{x=0} - \begin{pmatrix} 1 + m_e \alpha \hbar^{-2} \partial_x f \\ 1 - m_e \alpha \hbar^{-2} \partial_x g \end{pmatrix} = \frac{2mU_0}{\hbar^2} \Psi_{AM,e\uparrow}|_{x=0}. \quad (7)$$

and the charge current density

$$j_{Q,e(h)\sigma} = \text{Im}\{f^* \nabla f\} (-e\hbar/m_e \mp' e\alpha\sigma/\hbar) + \text{Im}\{g^* \nabla g\} (-e\hbar/m_e \pm' e\alpha\sigma/\hbar) \quad (8)$$

The boundary conditions for incident $e \downarrow$, $h \uparrow$ and $h \downarrow$ particles can be found in the SM. A similar procedure as described earlier can then be used to compute the charge and spin conductances of the junction.

The parameter Z characterizes the quality of electric contact between the AM and SC [18]. The high-transparency limit $Z \ll 1$ is routinely achievable experimentally using point-contact spectroscopy measurements [19, 20] or very high quality interfaces. A tunneling interface, modelled by $Z = 3$ in this work, can be achieved with the same experimental

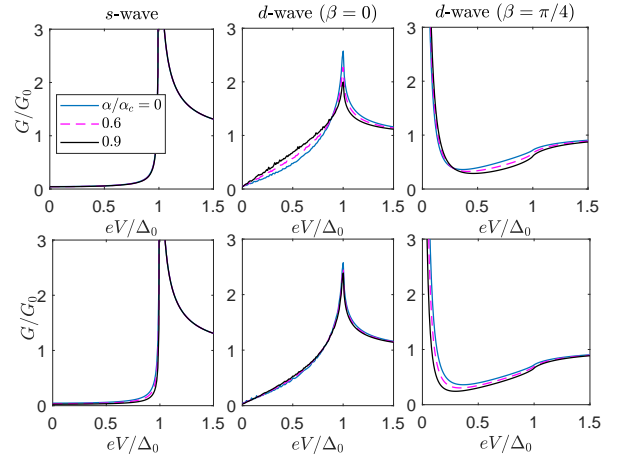


FIG. 3. (Color online) Normalized charge conductance G/G_0 as a function of bias voltage for different types of AM/SC junctions. The barrier is set to $Z = 3$, which describes a low-transparency contact. The columns correspond to different superconducting order parameter symmetries. *Upper row*: case (a) in Fig. 1 [AM term $\alpha k_x k_y$ in \underline{H}_{AM}]. *Lower row*: case (b) in Fig. 1 [AM term $\alpha(k_x^2 - k_y^2)/2$ in \underline{H}_{AM}].

technique by increasing the tip-sample distance or by explicitly inserting a thin insulator between the AM and SC. Both regimes of transport are of interest, and the altermagnetic interactions indeed reveal themselves differently in these two cases. The high-transparency case is shown in Fig. 2. In this case, increasing the magnitude of the spin-splitting α in the altermagnetic band structure substantially changes the conductance. In the s -wave and d -wave $\beta = 0$ cases, both known to not feature interfacial bound-states, the conductance is suppressed with increasing α . In the d -wave $\beta = \pi/4$ case, known to feature zero-energy bound states at interfaces and defects, the conductance is either enhanced or suppressed depending on the orientation of the spin-polarized elliptical Fermi-surfaces of majority and minority spin carriers.

The influence of altermagnetism on the conductance for the orientation shown in case (b) in Fig. 1 (corresponding to the lower row of Fig. 2) is similar to that of a conventional ferromagnet/superconductor junction: the magnetic interaction simply suppresses the conductance. This can be understood physically from the fact that the most dominant trajectories contributing to transport in the junction are the ones normal to the interface. For such directions of θ , the band-structure of the altermagnet is qualitatively similar to a ferromagnet in that one spin species dominates over the other independently of momentum.

Case (a) in Fig. 1 (corresponding to the upper row of Fig. 2) is more complex and interesting. In this case, there is no spin-polarization for normal incidence $\theta = 0$, while spin- \downarrow is the majority carrier for incident electrons with $\theta > 0$ and spin- \uparrow is the majority carrier for $\theta < 0$. The reduction in spin-polarization for incident particles then causes a lesser suppression of the charge conductance, consistent with the upper row of Fig. 2.

In Fig. 3, we show for completeness the case of a tunneling interface between the AM and SC. In this case, the altermagnetism has less effect on the charge conductance, even for large values $\alpha/\alpha_c = 0.9$. However, it is interesting to note that the zero-bias peak present for a d -wave $\beta = \pi/4$ order parameter [21, 22] survives for both orientations of the AM [case (a) and (b) in Fig. 1]. This suggests that the topological zero-energy states known to be present at d -wave interfaces are robust toward the presence of altermagnetism.

Finally, we consider the spin-polarization properties of the current flowing in the junction. For case (a) in Fig. 1, the spin conductance G_S is zero. This can be understood physically from the fact that the total spin polarization of the incident particles cancel since majority and minority spin bands swap for $\theta < 0$ and $\theta > 0$. Upon averaging over all incident angles, the spin polarization cancels.

For case (b) in Fig. 1, the transmitted current is spin polarized. The magnitude of the spin conductance G_S vanishes for $\alpha = 0$ and becomes very large compared to its normal-state value close to α_c . This is seen in the upper row of Fig. 4 with $Z = 0$: the spin conductance is enhanced by more than an order of magnitude for subgap voltages $eV < \Delta_0$ compared to the normal-state value $G_S(eV \gg \Delta_0)$. Moreover, the sign of the spin-polarization is tunable via the bias voltage eV in the case where surface-states exists (d -wave $\beta = \pi/4$). These properties make AM/SC attractive in terms of spin current control, since both the magnitude and the sign can be tuned *in situ* by the bias voltage. The low-transparency case is considered in the lower row of Fig. 4. Similarly to the charge conductance, the altermagnetic interaction has very little impact on the results in this case. Therefore, high-transparency contacts between altermagnets and superconductors will offer the clearest transport signature of the altermagnetic interaction.

In conclusion, we have shown that charge and spin conductances are strongly affected by altermagnetism for junctions with high-quality interfaces. The zero-energy states present for d -wave superconductors remain robust in the presence of altermagnetism, while the spin current can be enhanced by more than an order of magnitude and also change its sign depending on the applied bias voltage. Our predicted effects can be tested experimentally using a metallic altermagnet such as RuO_2 , and point the way toward further investigation of interesting spintronics effects in heterostructures comprised of altermagnets and superconductors.

Acknowledgments. S. Rex, J. Danon, A. Qaiumzadeh, and J. A. Ouassou are thanked for useful discussions. This work was supported by the Research Council of Norway through Grant No. 323766 and its Centres of Excellence funding scheme Grant No. 262633 “QuSpin.”

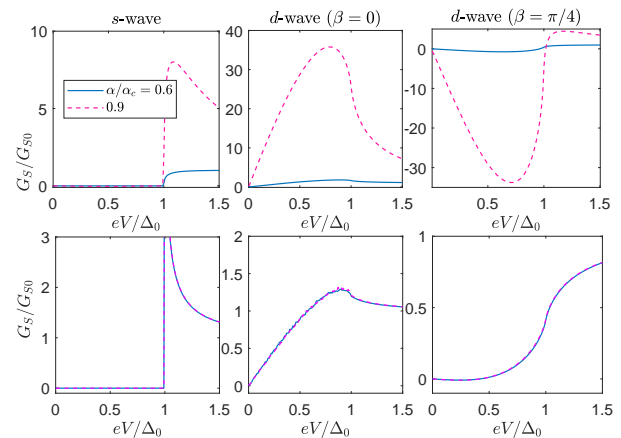


FIG. 4. (Color online) Normalized spin conductance G_S/G_{S0} as a function of bias voltage for case (b) in Fig. 1 [AM term $\alpha(k_x^2 - k_y^2)/2$ in $\underline{H}_{\text{AM}}$]. The columns correspond to different superconducting order parameter symmetries. *Upper row*: high-transparency contact $Z = 0$. *Lower row*: low-transparency contact $Z = 3$.

[1] F. S. Bergeret, A. F. Volkov, and K. B. Efetov Rev. Mod. Phys. **77**, 1321 (2005)
 [2] J. Linder and J. W. A. Robinson, Nat. Phys. **11**, 307 (2015)

[3] M. Eschrig, Rep. Prog. Phys. **78**, 104501 (2015)
 [4] A. I. Buzdin. Rev. Mod. Phys. **77**, 935 (2005).
 [5] F. S. Bergeret, M. Silaev, P. Virtanen, and T. T. Heikkilä Rev. Mod. Phys. **90**, 041001 (2018)
 [6] M. Amundsen, J. Linder, J. W. A. Robinson, I. Zutic, and N. Banerjee, arXiv: 2210.03549
 [7] A. F. Andreev, Sov. Phys. JETP. **19**, 1228 (1964).
 [8] K.-H. Ahn, A. Hariki, K.-W. Lee, and J. Kunes, Phys. Rev. B **99**, 184432 (2019)
 [9] S. Hayami, Y. Yanagi, and H. Kusunose, J. Phys. Soc. Jpn. **88**, 123702 (2019).
 [10] S. I. Pekar and E. I. Rashba. Zh. Eksp. Teor. Fiz. **47**, 1927 (1964).
 [11] L. Šmejkal, J. Sinova, and T. Jungwirth, Phys. Rev. X **12**, 040501 (2022).
 [12] L.-D. Yuan, Z. Wang, J.-W. Luo, E. I. Rashba, and A. Zunger. Phys. Rev. B **102**, 014422 (2020).
 [13] L. Šmejkal, R. González-Hernández, T. Jungwirth, and J. Sinova. Sci. Adv. **6**, 8809 (2020).
 [14] H. Reichlova, R.L. Seeger, R. González-Hernández, I. Kounta, R. Schlitz, D. Kriegner, P. Ritzinger, M. Lammel, M. Leiviskä, V. Petiček, P. Doležal, E. Schmoranzero, A. Badura, A. Thomas, V. Baltz, L. Michez, J. Sinova, S. T. B. Goennenwein, T. Jungwirth, and L. Smejkal. arXiv:2012.15651.
 [15] L. Šmejkal, J. Sinova, and T. Jungwirth, Phys. Rev. X **12**, 031042 (2022).
 [16] S. Lopez-Moreno, A. H. Romero, J. Mejia-Lopez, and A. Muñoz. Phys. Chem. Chem. Phys. **18**, 33250 (2016).
 [17] O. Fischer, M. Kugler, I. Maggio-Aprile, C. Berthod, and C. Renner. Rev. Mod. Phys. **79**, 353 (2007).
 [18] G. E. Blonder, M. Tinkham, and T. M. Klapwijk Phys. Rev. B **25**, 4515 (1982).
 [19] Y. G. Naidyuk and I. K. Yanson, *Point-Contact Spectroscopy*, Springer Series in Solid-State Sciences **145** (Springer, 2004)
 [20] D. Daghero, R.S. Gonnelli Supercond. Sci. Technol. **23** 043001 (2010)
 [21] C.-R. Hu, Phys. Rev. Lett. **72**, 1526 (1994)
 [22] Y. Tanaka and S. Kashiwaya, Phys. Rev. Lett. **74**, 3451 (1995).